Quaternary Geochronology 30 (2015) 438–444

Contents lists available at ScienceDirect

Quaternary Geochronology

journal homepage: www.elsevier.com/locate/quageo

Research paper

Feldspar multi-elevated-temperature post-IR IRSL dating of the Wulanmulun Paleolithic site and its implication

Xue Rui [a], Jia-Fu Zhang [a, *], Ya-Mei Hou [b], Ze-Meng Yang [c], Yang Liu [c], Zi-Ming Zhen [c], Li-Ping Zhou [a]

[a] MOE Laboratory for Earth Surface Processes, Department of Geography, College of Urban and Environmental Sciences, Peking University, Beijing 100871, China
[b] Institute of Vertebrate Paleontology and Paleoanthropology, Chinese Academy of Sciences, Beijing 100044, China
[c] Ordos Antiquity & Archaeology Institution, Ordos, Inner Mongolia Autonomous Region 017200, China

ARTICLE INFO

Article history:
Received 7 November 2014
Received in revised form
20 April 2015
Accepted 5 May 2015
Available online 15 May 2015

Keywords:
Potassium feldspar
Luminescence dating
MET-pIRIR procedure
Residual dose subtraction
Preheat plateau
Extended age plateau
Wulanmulun Paleolithic site

ABSTRACT

The Wulanmulun site found in 2010 is an important Paleolithic site in Ordos (China), from which lots of stone and bone artifacts and mammalian fossils have been recovered. It was previously dated by radiocarbon and optically stimulated luminescence (OSL) techniques on quartz. To further confirm the reliability of the chronology constructed based on OSL ages and test the applicability of the recently developed pIRIR procedure on sediments from northern China, twenty-four sediment samples (including eolian, lacustrine and fluvio-eolian sands) from the site were determined using the multi-elevated-temperature post-IR IRSL (MET-pIRIR or pIRIR) procedure on potassium feldspar. The results show that the studied samples have two MET-pIRIR D_e preheat plateaus (280–320 and 340–360 °C), and the bleaching rates of the luminescence signals are associated with sample ages and stimulation temperatures. All the pIRIR ages (7–155 ka) corrected for anomalous fading and residual dose obtained after solar bleaching for 15 h are larger than the corresponding quartz OSL ages (4–66 ka) previously determined, even for the young eolian samples (<10 ka). But the corrected IRSL(50 °C) ages (6–85 ka) are broadly consistent with the quartz ages. It appears that the IRSL(50 °C) ages are more reliable, although this contradicts the previously results obtained by other people. On the other hand, we also obtained an extended age plateau between the stimulation temperatures of 50 and 290 °C in the plot of age versus stimulation temperature (A-T plot) by subtracting different residual doses obtained after different bleaching times. The reliability of the plateau ages requires further investigation. For the sediment samples from this site, quartz should be more suitable for dating than K-feldspar, and the quartz OSL ages of 50–65 ka for its cultural layer should be reliable.

1. Introduction

Quartz as a sensitive and reliable natural dosimeter has been widely used in optically stimulated luminescence (OSL) dating of sediments in the past decades. However, quartz OSL ages might be underestimated due to relatively low saturation dose of quartz signals (Wintle and Murray, 2006), non-fast components (Choi et al., 2003; Li and Li, 2006; Tsukamoto et al., 2007) or unstable fast components (Murray and Funder, 2003; Fan et al., 2011). Potassium feldspar (K-feldspar) as an alternative dosimeter for OSL dating has relative high saturation dose and is brighter than quartz, but the possible presence of anomalous fading has limited its wider application (Wintle, 1973; Spooner, 1994). To solve this problem, two approaches have been suggested. One is to make fading correction (e.g. Huntley and Lamothe, 2001), and the other is to obtain non-fading components such as post-IR IRSL (pIRIR) signals (e.g. Thomsen et al., 2008; Li and Li, 2011). Based on K-feldspar pIRIR signals, two steps (Thomsen et al., 2008) and multi-elevated-temperature post-IR IRSL (MET-pIRIR) procedures (e.g. Li and Li, 2011) have been proposed. These new methods have been widely investigated in recent years, and have potential for routine dating of sediments (see review by Li et al., 2014a).

The chronology of the Wulanmulun Paleolithic site in Ordos is considered essential for understanding the significance of the

* Corresponding author.
E-mail address: jfzhang@pku.edu.cn (J.-F. Zhang).

http://dx.doi.org/10.1016/j.quageo.2015.05.004
1871-1014/

excavated artifacts. The site has been dated using radiocarbon and quartz OSL techniques, the results will be presented in a separate paper. The results indicate that the ages of the cultural layers are beyond the upper limit of the radiocarbon dating. Here, we applied the recently developed MET-pIRIR procedure (Li and Li, 2011, 2012; Fu et al., 2012a; Fu and Li, 2013) to this site. The aims are to check the applicability of this method on the site deposits including eolian, fluvio-eolian and lacustrine sediments, and to confirm the reliability of the chronology established by quartz OSL dating. In this study, extensive laboratory tests (preheat plateau, dose recovery, bleaching, fading and IR-off) have been performed.

2. Geological setting, archaeology and sampling

The Wulanmulun Paleolithic site found in 2010 is located in the north bank of the Wulanmulun River in the Dongsheng district of Ordos, Inner Mongolia Autonomous Region, China (Fig. 1). This site is considered as another new important discovery of prehistoric culture in Ordos region after the Salawusu (Sjaraosso-gol) (Boule et al., 1928) and Shuidonggou (Teilhard de Chardin and Licent, 1924) sites discovered by French researchers in 1922 (Hou et al., 2012; Wang et al., 2012). The site consists of three localities, Locality 1 (39°35′03.48″N, 109°45′41.97″E) studied in this paper is situated in a paleovalley on the bank of the river. The paleovalley is filled with eolian, fluvio-eolian and lacustrine sediments. Based on field observation, the site deposits are divided into upper and lower units (Fig. S1). The upper unit is (around 10 m thick) composed of eolian sands and lake sediments. The lower unit is further divided into eight stratigraphic layers (marked from top to bottom as Layers 1–8). Layer 1 (1.1–2.1 m thick) consists of red eolian sand including small rock debris. Layer 2 (0.6–1.4 m) is composed of red sand and grey silt. Layer 3 (0.3–0.8 m) is red fine sand intercalated with grey fine sand. Layer 4 (0.2–0.6 m) is grey silt. Layer 5 (0.15–0.4 m) is composed of grey silt and red fine sand. Layer 6 (0.6–0.8 m thick) is red fine sands including rock debris. Layer 7 (0.2–0.4 m) is grey silt. Layer 8 (1.1–2.1 m) is composed of red fine sand intercalated with grey silt overlying the bedrock of Cretaceous red eolian sandstones.

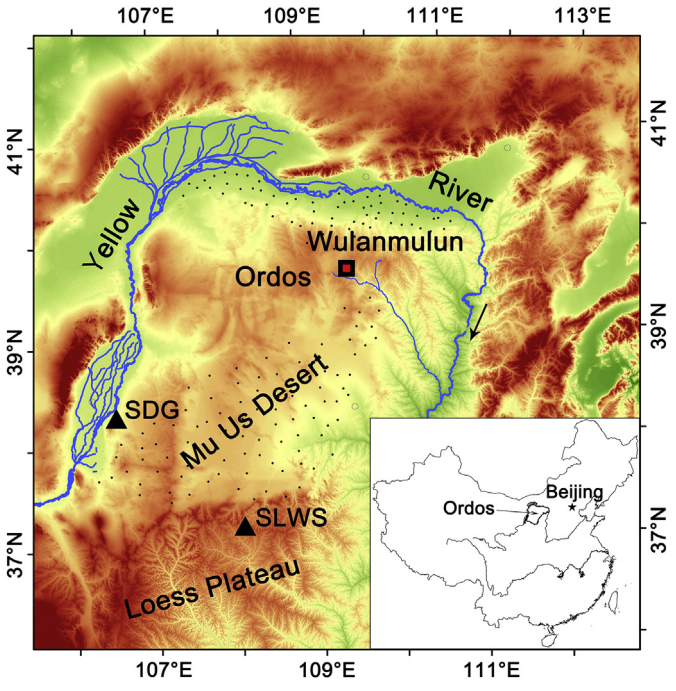

Fig. 1. Map showing the location of the Wulanmulun, Salawusu (SLWS) and Shuidongou (SDG) Paleolithic sites in Ordos.

Various stone and bone artifacts were found from the cultural unit consisting of Layers 2–8. They include cores, blades, assorted tools and flakes (Hou et al., 2012; Wang et al., 2012). Around 65% of the stone artifacts are blades, and 90% of the stone artifacts are made from sandstones. Assorted tools include scrapers, end scrapers and points. Excavations yielded various mammalian fossils, mainly composed of *Coelodonta antiquitatis*, *Equus przewalskii* and *Megaloceros ordosianus* (Dong et al., 2014). Large dense of charcoal and burnt bones were excavated from Layers 2, 5 and 6 (Wang et al., 2012).

A total of 24 samples were collected for luminescence dating. Nine samples (eolian sands and lacustrine sediments) were taken from the upper unit, 15 samples (lacustrine and fluvio-eolian samples) were from the lower unit. In order to compare the luminescence properties, two samples were taken from bedrock. All luminescence samples except for bedrock samples were collected by hammering stainless steel tubes on the section. The sampling depth and description of each sample are listed in Table S1.

3. Methodology

All samples were treated in a dark room with subdued red light. The potentially light-exposed sediments of 2-cm thickness at both ends of sampling tubes were first removed, and used for dose rate measurement, assuming that the samples are homogeneous. The interior samples were treated with 10% HCl and 10% H_2O_2 to remove carbonates and organic material, respectively. The samples were then dry sieved, and the size of the grains obtained for OSL measurements are shown in Table S1. The heavy liquid (a sodium polytungstate) with a density of 2.58 g/cm^{-3} was used to separate K-feldspar grains from the samples. The K-feldspar samples were etched using 10% HF for 40 min to remove the alpha irradiated outer layer, and then using 10% HCl to remove fluorides formed during HF etching. The K-feldspar grains obtained were mounted as a monolayer on 9.8 mm aluminum discs using silicone oil as an adhesive, medium aliquots (~5 mm in diameter) were created for OSL measurements.

The MET-pIRIR procedure proposed by Li and Li (2011) was used for equivalent dose (D_e) measurements. Here, the procedure (Table S2) includes four-step IR stimulations at temperatures of 50, 150, 220 and 290 °C. Preheat of 300 °C for 60 s (determined from preheat plateau tests) was used, and test doses of 10–30 Gy were applied. A high-temperature bleach at 325 °C for 100 s was conducted at the end of each round of the measurement to make a low residual signal for the next cycle. In the OSL decay curves, the counts of the first 2 s integral after subtracting the last 10 s integral which assumed as the background was used for D_e calculation. All luminescence measurements and irradiation were carried out with an automated Risø TL-DA-15 reader. IR diodes (870 ± 40 nm) were performed for stimulation (Bøtter-Jensen et al., 2003). The luminescence signals were detected using EMI 9235QA photomultiplier tube which equipped with a filter pack of Schott BG-39 and Corning 7–59 filters, providing a blue transmission window (320–480 nm).

In order to determine the stimulation time in the MET-pIRIR procedure (Table S2), two stimulation times were first tested using the procedure on sample L1810. The decay curves for the IRSL (50 °C) and pIRIR signals shown in Fig. S2 do not reach a constant level after 100 s or 200 s of stimulation, and the signals continue to decay. Additionally, the D_e values obtained using both the stimulation times are identical. In this case, 100 s stimulation was applied in our samples in order to save measurement time. In order to observe the effect of isothermal thermoluminescence (TL) on elevated temperature pIRIR signals and the thermal transfer (Qin and Zhou, 2012; Wang and Wintle, 2013; Wang et al., 2014), an 'IR-off' period of 20–100 s was applied before IR stimulations (Fu

et al., 2012a). 'IR-off' periods of 10–40 s were also performed after IR stimulations to detect the residual isothermal TL signals. The results (Fig. S3) show that the isothermal TL signals are negligible compared to the IRSL(50 °C) and pIRIR signals, suggesting that the isothermal TL signals had little effect on pIRIR signals. The 'IR-off' step was thus not conducted during D_e measurements in this study.

The U, Th and K contents of the samples were measured by neutron-activation-analysis (NAA), and secular equilibrium in the U and Th decay series in the sediments are assumed. The burial depth was used to calculate the contribution from cosmic ray (Prescott and Hutton, 1994). The internal K-content of the K-feldspar grains was assumed to be 13 ± 1% (Huntley and Baril, 1997; Zhao and Li, 2005; Li et al., 2008). Water contents were determined by measuring the sample weights before and after drying. The 'AGE' program of Grün (2009) was used to convert the elemental concentrations into effective dose rates.

4. Results and discussion

4.1. Luminescence properties

4.1.1. Dose response curves

The dose response curves (DRCs) for four representative samples are illustrated in Fig. 2. The curves are fitted with a single exponential saturation function, and the 'characteristic saturation dose' D_0 value (Wintle and Murray, 2006) calculated for each curve is also shown in the figure. It shows that the signals of 50, 150 and 220 °C from one sample have similar D_0 values, while a lower D_0 value is observed for the signal of 290 °C. Fig. 2 also demonstrates that the D_0 value increases with sample age, and the bedrock sample (JY-2) has the highest value. The D_e values obtained from each signal are far less than the corresponding $2D_0$ values, indicating that the natural signals are far away from saturation. Additionally, the recycling ratios for all signals from all samples are within the range of 1.0 ± 0.1 and the recuperations all less than 5%, suggesting that the sensitivity correction for these samples is successful and thermal transfer negligible.

4.1.2. Preheat plateau

A preheat plateau test on sample L2095 was carried out to determine a suitable preheat temperature for D_e measurements. D_e values were measured using the procedure in Table S2 with different preheat temperatures ranging from 280 to 360 °C in step of 20 °C. For each temperature, three aliquots were measured. The plot of D_e values against preheat temperatures (Fig. 3) shows that two preheat plateaus (280–320 and 340–360 °C) can be recognized. It can be seen that the D_e values obtained in the preheat temperatures of 280–320 °C are larger than those for the temperatures of 340–360 °C. Similar pIRIR D_e plateaus were also found for the terrace deposits of the Yellow River (Meng et al., 2015). But these are contrary to the results of Roberts (2012) who found that the pIRIR D_e values for her loess samples have a plateau at the preheat temperature range of 250–280 °C, but increase significantly from 280 to 320 °C. However, Li and Li (2011) reported a pIRIR D_e plateau over the preheat temperature range of 220–300 °C for their aeolian samples (~12 ka) from northern China. These imply that the preheat dependence of D_e is sample dependent. Based on the fact that the preheat temperature ≤320 °C are usually used in feldspar pIRIR dating (e.g. Buylaert et al., 2009; Murray et al., 2009; Thiel et al., 2011; Li and Li., 2011) and the preheat plateau in Fig. 3, the preheat of 300 °C for 60 s was used in this study.

4.1.3. Dose recovery

A dose recovery test was also performed on four samples. In this test, three aliquots of each sample were first bleached for 8 h with a solar simulator (Dr. Hönle UVACUBE 400), and then given a laboratory beta dose equivalent to the pIRIR (290 °C) D_e value of the measured sample. The given dose was then measured as an 'unknown' dose using the procedure in Table S2 with preheat temperature of 300 °C. The ratios of measured to given dose (dose recovery ratio) for the signals are shown in Fig. 4. It indicates that the ratios are lowest for IRSL (50 °C) signal (between 0.63 ± 0.04 for sample L2095 and 0.75 ± 0.08 for L1816) and increase with temperature until 290 °C (between 0.97 ± 0.04 for L1798 and 1.3 ± 0.1 for L1815), regardless of whether the sample is eolian (L1797 and 2095) or waterlain (L1815 and 1816). The ratios for the pIRIR (150 °C) and (220 °C) signals are generally within 1.0 ± 0.1 at 1σ. Compared to the ratios for other samples from different regions (see review by Li et al., 2014a), the ratios for our samples are acceptable. On the other hand, the dose recovery ratios may be unimportant to predict inaccurate D_e estimation (Buylaert et al., 2012).

4.1.4. Residual doses after bleaching

A bleaching test was carried out on three samples (L1798, 2096 and 1816) using the solar simulator. In this test, the natural aliquots were measured using the procedure in Table S2 after exposure to

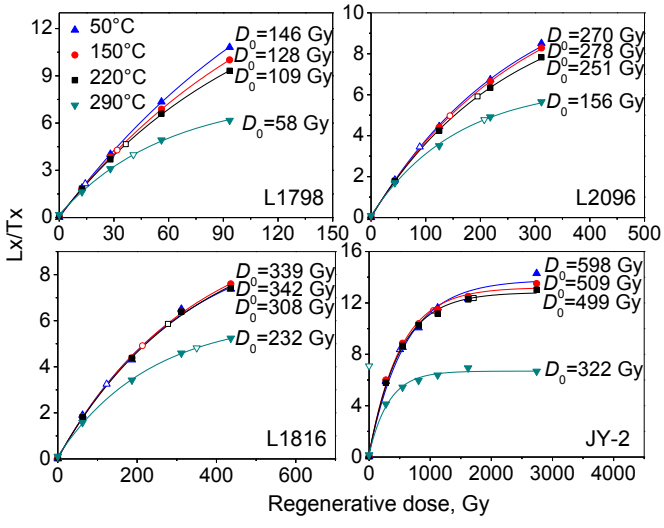

Fig. 2. Dose-response curves of the IRSL(50 °C) and MET-pIRIR (150, 220 and 290 °C) signals for four representative samples. The D_0 values calculated using the equation $I = I_0(1\text{-}exp(-x/D_0))$ for the curves are also labeled. The open points represent the sensitivity-corrected (Lx/Tx) natural signals.

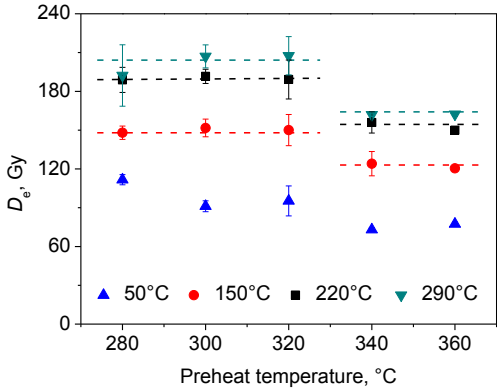

Fig. 3. Effect of preheat temperature on IRSL(50 °C) and MET-pIRIR D_e values for sample L2095. Each data point represents the average of three aliquots, and error bars for some points fall within the data symbols.

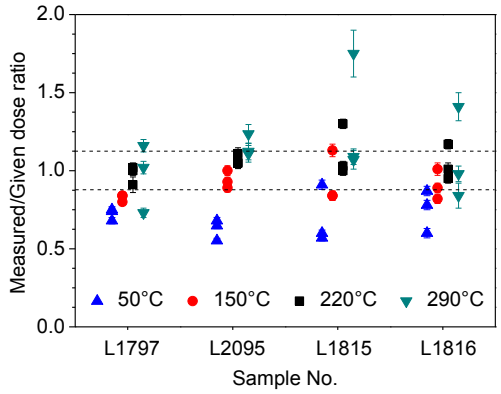

Fig. 4. Results of dose recovery tests for four samples. Each data point represents an estimate from an individual aliquot.

the solar light for periods ranging from 1 to 900 min. Three aliquots were performed for each bleaching time. The results are shown in Fig. 5. It can be seen that after 900 min bleaching, the remaining doses from the high-temperature pIRIR signals are larger than those from the low-temperature pIRIR signals, and all the pIRIR doses are larger than the corresponding IRSL(50 °C) dose, reflecting

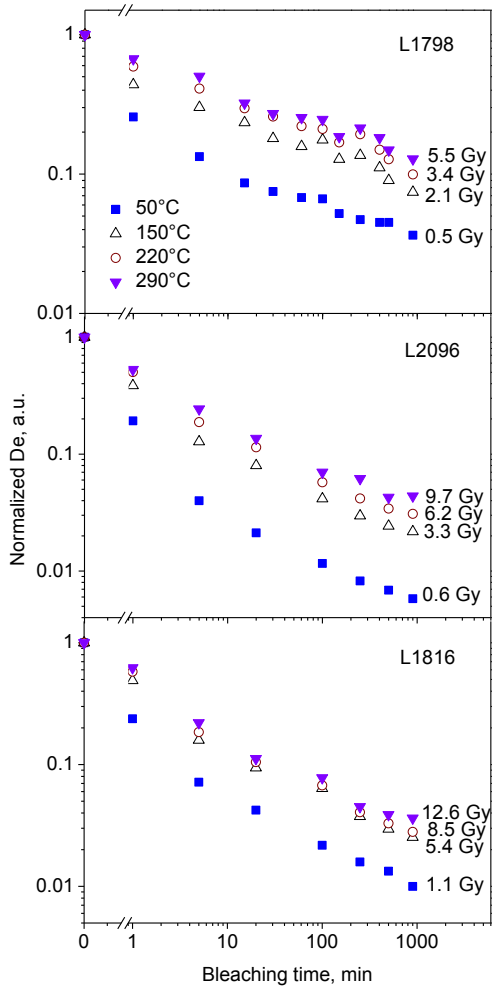

Fig. 5. Residual doses measured after different bleaching times using a solar simulator for three representative samples. In order to compare, all doses are normalized to the natural D_e values (0 min bleaching time). Each data point represents the average of the results from three aliquots, the associated errors are not shown for clarity. The doses remaining after 900 min bleaching for each signal are labeled.

their different bleachability. On the other hand, it appears that the residual doses are associated with sample ages, that is, the residual doses for the older samples (L2096 and L1816) are larger than those for the young sample (L1798). This is similar to the results reported by previous investigators (e.g., Sohbati et al., 2012; Buylaert et al., 2012; Schatz et al., 2012), but contrary to the results of Li et al. (2013) who considered that there is no clear relationship between the size of residual dose and sample ages for their samples. Fig. 5 also demonstrates that the remaining doses determined after 500 min bleaching are very close to those obtained after 900 min bleaching, implying that the pIRIR signals corresponding to the most part of the residual doses measured after 900 min bleaching may consist of the less bleachable and non-bleachable signals and those induced by thermal transfer of charge from light-insensitive traps to those associated with the IRSL (50 °C) and pIRIR signals (Buylaert et al., 2012; Li et al., 2014a). Such residual doses should be subtracted from the D_e values before age calculation.

4.1.5. Anomalous fading

Anomalous fading rates were measured on three samples (L1797, L1802 and L1815) using the procedure similar to that described by Auclair et al. (2003), but signal measurement based on the procedure of Table S2. The results (Fig. S4) show that the three samples have similar anomalous fading rates. The average g-values for the IRSL (50 °C), pIRIR(150 °C), pIRIR(220 °C) and pIRIR(290 °C) signals from the three samples are 4.5 ± 0.1, 2.1 ± 0.1, 1.8 ± 0.3 and 0.8 ± 0.1%/decade, respectively. The rates for the pIRIR signals decrease with increasing stimulation temperature as reported by Li and Li (2011, 2012), and the rate of the pIRIR(290 °C) signal is negligible.

4.2. Dating results

4.2.1. De values and IRSL(50 °C) and MET-pIRIR ages corrected for anomalous fading and non-bleachable signals

The calculated dose rates of the studied samples are listed in Table S1. They range from 3.6 to 2.9 Gy/ka, with an average of 3.23 ± 0.04 Gy/ka, and the average internal dose rate is about 21% of the sample-average total dose rate. The IRSL(50 °C) and pIRIR D_e values obtained for each sample are listed in Table S3. It is shown that the measured D_e values increase with increasing stimulation temperature, that is, the IRSL(50 °C) D_e < pIRSL(150 °C) D_e < pIRSL(220 °C) D_e < pIRIR (290 °C) D_e, this can be explained by the differences in anomalous fading rate and residual dose between the signals. The pIRIR (220 °C) D_e values for the bedrock samples are up to 1800 Gy, and the pIRIR (290 °C) D_e values more than 2750 Gy, which are greatly larger than those of the sediment samples, implying that the ages of the studied sediment samples are far less than the upper age limit of the pIRIR method.

As discussed above, the studied samples suffered from anomalous fading, and have residual doses which most likely result from non-bleachable signals and/or thermal transfer. This means that the directly measured D_es should be corrected for before age calculation. Here the residual doses obtained after 900 min of solar bleaching were first subtracted from the measured D_es, and then the residual-subtracted D_e values were corrected for anomalous fading (Huntley and Lamothe, 2001). It is noted that the residual doses (obtained from samples L1798, L2096 and L1816) and g-values (obtained from samples L1797, L1802 and L1815) were used for relatively young samples (L1797-L1801), eolian samples (L1802-L1805, L2095 and L1906) and lacustrine and fluvio-eolian samples (L1806-1818), respectively. The IRSL(50 °C) and pIRIR ages corrected for both residual dose and anomalous fading for the studied samples are listed in Table S3. One example of the plots of age against stimulation temperature (A-T plot) is shown in Fig. 6. It can be seen that the corrected IRSL(50 °C) age values are smallest, and

an age plateau can be observed between the stimulation temperatures of 220 and 290 °C within errors. Such age plateau in the A-T plot is usually used to assess the effect of anomalous fading, bleaching and thermal transfer on ages. If an age plateau in the A-T plot is achieved, the plateau age is consider reliable (Li and Li, 2011; Li et al., 2013, 2014b; Fu et al., 2012a). Based on this criteria, the pIRIR(220 °C) and pIRIR(290 °C) ages obtained for our samples appear to be reliable.

4.2.2. The reliability of the IRSL(50 °C) and MET-pIRIR ages corrected for anomalous fading and non-bleachable signals

In order to further assess the reliability of the IRSL(50 °C) and pIRIR ages corrected for both anomalous fading and non-bleachable signals, the corrected ages are compared to their corresponding quartz OSL ages (the quartz OSL dating of the site will be presented separately by the authors) in Fig. 7a. It can be seen that all the IRSL(50 °C) ages are in agreement with their corresponding quartz OSL ages, and all the pIRIR ages are greatly larger than the quartz ages. It appears that the corrected IRSL(50 °C) ages may be reliable for our samples, although the dose recovery ratios for this signal are much less than 1. However, the above discussion suggested that the pIRIR(220 °C) and pIRIR(290 °C) ages should be reliable, and consistent with the quartz OSL ages. For the inconsistency between quartz OSL and pIRIR ages, there may be a possibility that the quartz OSL ages were underestimated. This is because the OSL ages of some quartz samples from Mu Us Desert located to the south of the Wulanmulun site (Fig. 1) seem to be underestimated (Fan et al., 2011). However, the unstable fast OSL component of quartz grains and the fact that the uncorrected IRSL(50 °C) ages for the samples are less than the corresponding quartz OSL ages for their quartz samples were not observed in our samples. In addition, the low dose saturation characteristics of quartz may also result in the underestimation of older samples. However, the corrected pIRIR ages for younger eolian samples (for example, sample L1798 with quartz OSL age of ~4 ka) from the upper unit are still larger than their corresponding quartz OSL ages. Therefore, there is no evidence to support the fact that the quartz OSL ages of the studied samples were systematically underestimated. In this case, we infer that the pIRIR ages corrected for anomalous fading and less-bleachable and non-bleachable signals obtained after 900 min of bleaching should be overestimated.

It is known that feldspar luminescence is bleached more slowly than OSL quartz signals (Godfrey-Smith et al., 1988; Thomsen et al., 2008), and elevated-temperature pIRIR signals have relatively slow bleaching rates (e.g. Li and Li, 2011; Buylaert et al., 2012; Fu et al., 2012b), as shown in Fig. 5 and Fig. S2. Thus, we deduce that the overestimation of the K-feldspar pIRIR ages should be partly attributed to the relatively poor bleaching of the pIRIR signals prior to deposition. The residual pIRIR doses obtained after 900 min bleaching in laboratory could not represent the inherited dose remaining from the earlier period of burial. On the other hand, the difference between the quartz OSL and corresponding pIRIR ages generally increases as the samples become older (increasing depth) (Fig. 7a). For example, samples L1798, L2096 and L1816 yielded quartz OSL ages of 4.0 ± 0.4, 45.4 ± 2.1 and 56.3 ± 3.5 ka, and K-feldspar pIRIR (290 °C) ages of 11.5 ± 2.3, 69.8 ± 7.7 and 107.4 ± 17.1 ka, respectively. The differences between the quartz OSL and K-feldspar pIRIR(290 °C) ages for the three samples are 7.5 (corresponding to 24 Gy of K-feldspar) ka, 24.4 (73 Gy) ka and 51.1 (168 Gy) ka, respectively. If we assume that the age differences are completely attributed to incomplete bleaching of K-feldspar, the bleaching level would decrease with increasing sample ages (depth). Based on the age difference, sample L2096 was much more poorly bleached than L1798 at deposition, given the same eolian depositional environment, and the degree of bleaching of sample L1816 is 7 times lower than L1798. Obviously, it is difficult to believe that this is the case, and there is no reason why the older samples have much larger residual dose than the young ones at the time of deposition. Thus, we deduce that the overestimation of the pIRIR ages for our samples are partly due to the thermal transfer as discussed above, and the dose inherited from source materials and induced by the thermal transfer occurring during measurement should thus be responsible for the overestimation of the pIRIR ages. Therefore, the simple subtraction of the residual dose of less-bleaching and non-bleaching pIRIR signals obtained in the bleaching tests from the measured D_e values does not yield reliable pIRIR ages for our samples. Another factor leading the pIRIR age overestimation may be the unsuitable preheat temperature of 300 °C used during the D_e measurement (Fig. 3), which requires further investigation.

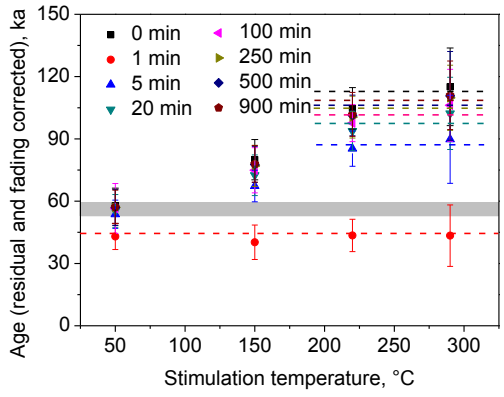

Fig. 6. Plot of age versus stimulation temperature for sample L1816. The IRSL(50 °C) and pIRIR ages are corrected for anomalous fading and residual doses obtained after different bleaching times (0–900 min) in the laboratory. The grey shaded region refers to the corresponding quartz OSL age, and the dashed lines represent age plateaus.

4.2.3. Performance of residual dose correction

The size of residual dose for pIRIR signals remaining even after long bleaching time in a solar simulator or daylight (for modern sample) is known to vary significantly from sample to sample (Fig. 5, and see review by Li et al., 2014a). The measured D_es should be corrected for residual dose before age calculation. There have been two correction methods: residual dose subtraction (e.g., Thomsen et al., 2008; Li and Li, 2011) such as in Section 4.2.1 and residual signal intensity subtraction (Li et al., 2013; Schmidt et al., 2014). Li et al. (2013) considered that the simple dose-subtraction method will result in a significant underestimation of the actual burial dose. But the application of this method to our samples showed that this is not the case (see Section 4.2.1). They further argue that the intensity-subtraction method will yield relative larger D_e value than the dose-subtraction method. Therefore, we do not apply the intensity-subtraction method to our samples.

The residual dose obtained from bleaching tests and modern samples should consist of three components corresponding to bleachable and non-bleachable signals, and that induced by thermal transfer during measurement. The residual dose (RD1) obtained after long bleaching times such as 900 min would be dominated by the contribution from non-bleachable signals and those from thermal transfer. If RD1 is used for correction, the corrected D_e values may be larger than the actual burial dose. This is because the residual dose (RD2) responsible for bleachable signals are not subtracted from the total measured D_e. However, it is difficult to quantify the level of RD2 at the time of deposition. Fig. 6 and Fig. 5s demonstrate the IRSL(50 °C) and pIRIR ages corrected for anomalous fading and residual doses (RD1+RD2) obtained after different laboratory

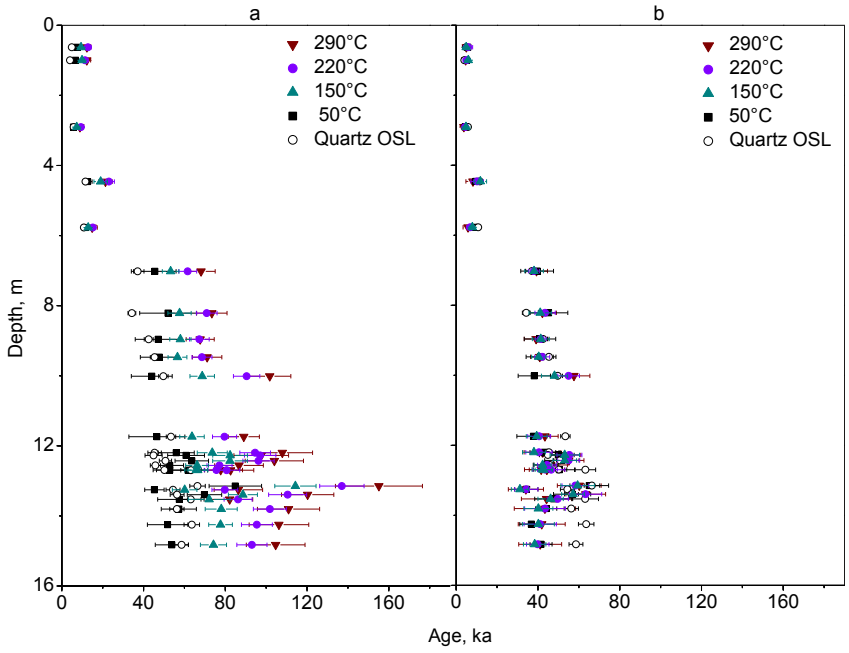

Fig. 7. Plots of the IRSL(50 °C) and pIRIR ages corrected for both anomalous fading and residual dose versus sample depth. (a) The residual dose for each signal was obtained after 15 h bleaching, and (b) the residual doses were determined based on the extended age plateau between all stimulation temperatures (see text for details and Fig. 6 and Fig. S5). The corresponding quartz OSL ages are also presented for comparison.

bleaching times. It is noted that the residual doses after different bleaching times for other samples (except for bleaching samples (L1798, L2096 and L1816)) were calculated based on the functions fitted to the data in Fig. 5. From the A-T plots in Fig. 6 and Fig. 5s, it can be seen that an age plateau between stimulation temperatures of 220 and 290 °C can be observed for each bleaching time if error bars are considered. Each plateau corresponds to a different degree of bleaching of a sample. It is difficult to determine which degree of bleaching is true for the sample at the time of deposition based only on the plateaus. Fig. 6 and Fig. S5 also show that the IRSL(50 °C) and all pIRIR ages corrected for the dose remaining after suitable bleaching times such as 1 or 1.5 min are identical, constructing an age plateau between stimulation temperatures of 50 and 290 °C. This means that an extended age plateau between all the stimulation temperatures can be achieved for a sample, if suitable residual doses for the IRSL and pIRIR signals are used for correction. As shown in Fig. 5, the different signals have different bleaching rates, so the extended plateau may imply that the correction for both anomalous fading and residual dose are successful. After such correction, the agreement between the IRSL (50 °C) and pIRIR ages were also found for other samples (e.g. Buylaert et al., 2009; Trauerstein et al., 2014).

The extended plateau ages for each signal are also plotted as a function of sampling depth in Fig. 7b. It is shown that the plateau ages of 16 samples are consistent with their corresponding quartz OSL ages. This implies that the plateau ages may represent the true burial ages of the studied samples. However, the ages of the other 8 samples are younger than the corresponding quartz OSL ages, especially for the relatively old samples below the depth of 12.69 m. For these relatively old samples, the anomalous fading may not be successfully corrected (Huntley and Lamothe, 2001) although the extended age plateaus are reached, and result in the underestimation of the plateau ages. For such samples, further investigations are very necessary.

5. Conclusion

The IRSL(50 °C), pIRIR(150 °C), pIRIR(220 °C) and pIRIR(290 °C) signals measured using successive IR stimulations at sample temperatures of 50, 150, 220 and 290 °C after preheating or cutheating demonstrate different properties. The pIRIR signals have relatively lower saturation dose and slower bleaching rate than the IRSL(50 °C) signal, and the anomalous fading of the pIRIR(290 °C) signal is negligible. The doses remaining after long bleaching times appear to be associated with sample age and stimulation temperature. The preheat temperature in the MET-pIRIR procedure on K-feldspar may be crucial for an accurate D_e estimation. The IRSL(50 °C) ages corrected for anomalous fading and residual dose obtained after 15 h bleaching in a solar simulator are broadly consistent with the corresponding quartz OSL ages, but all the corrected pIRIR ages are larger than the quartz ages, even for the young (<10 ka) eolian samples. This result contradicts the previously published dating studies in which the pIRIR ages are considered more reliable. In this study, an extended age plateau between stimulation temperatures of 50 and 290 °C in the plot of age versus stimulation temperature can be achieved for a sample by correcting for anomalous fading and a series of residual doses measured after different bleaching times. The relatively young samples have the plateau ages consistent with the corresponding quartz OSL ages, but the relatively old samples yielded relatively younger plateau ages. The reliability of the plateau ages requires further investigation. The application of the MET-pIRIR procedure to the Wulanmulun site is complicated by the luminescence properties of the studied samples. We thus consider that quartz is more suitable for dating than K-feldspar for this site, and the quartz OSL ages of 50–65 ka for its cultural layer should be reliable.

Acknowledgments

The work was supported by the National Natural Science Foundation of China (NSFC, Nos.: 41171007 and 41272033), Special Funds for Scientific Research on Common Weal Profession of MLR (No. 20121105–3) and the CAS Strategic Priority Research Program Grant (No. XDA05130203). We are grateful to the anonymous reviewer, his/her valuable comments and constructive suggestions

significantly improved the quality of the manuscript.

Appendix A. Supplementary data

Supplementary data related to this article can be found at http://dx.doi.org/10.1016/j.quageo.2015.05.004.

References

Auclair, M., Lamothe, M., Huot, S., 2003. Measurement of anomalous fading for feldspar IRSL using SAR. Radiat. Meas. 37, 487–492.

Bøtter-Jensen, L., Andersen, C.E., Duller, G.A.T., Murray, A.S., 2003. Developments in radiation, stimulation and observation facilities in luminescence measurement. Radiat. Meas. 37, 535–541.

Boule, M., Breuil, H., Licent, E., Teilhard de Chardin, P., 1928. Le Paleolithique de la Chine. Masson et cie. Editeurs, Paris.

Buylaert, J.P., Jain, M., Murray, A.S., Thomsen, K.J., Thiel, C., Sohbati, R., 2012. A robust feldspar luminescence dating method for Middle and Late Pleistocene sediments. Boreas 41, 435–451.

Buylaert, J.P., Murray, A.S., Thomsen, K.J., Jain, M., 2009. Testing the potential of an elevated temperature IRSL signal from K-feldspar. Radiat. Meas. 44, 560–565.

Choi, J.H., Murray, A.S., Cheong, C.S., Hong, D.G., Chang, H.W., 2003. The resolution of stratigraphic inconsistency in the luminescence ages of marine terrace sediments from Korea. Quat. Sci. Rev. 22, 1201–1206.

Dong, W., Hou, Y.M., Yang, Z.M., Zhang, L.M., Zhang, S.Q., Liu, Y., 2014. Late Pleistocene mammalian fauna from Wulanmulun Paleolithic site, Nei Mongol, China. Quat. Int. 347, 139–147.

Fan, A., Li, S.H., Li, B., 2011. Observation of unstable fast component in OSL of quartz. Radiat. Meas. 46, 21–28.

Fu, X., Li, S.-H., 2013. A modified multi-elevated-temperature post-IR IRSL protocol for dating of Holocene sediments using K-feldspar. Quat. Geochronol. 13, 44–54.

Fu, X., Li, B., Li, S.H., 2012a. Testing a multi-step post-IR IRSL dating method using polymineral fine grains from Chinese loess. Quat. Geochronol. 10, 8–15.

Fu, X., Zhang, J.F., Zhou, L.P., 2012b. Comparison of the properties of various optically stimulated luminescence signals from potassium feldspar. Radiat. Meas. 47, 210–218.

Godfrey-Smith, D.L., Huntley, D.J., Chen, W.H., 1988. Optically dating studies of quartz and feldspar sediment extracts. Quat. Sci. Rev. 7, 373–380.

Grün, R., 2009. The "AGE" program for the calculation of luminescence age estimates. Anc. TL 27, 45–46.

Hou, Y.M., Wang, Z.H., Yang, Z.M., Zhen, Z.M., Zhang, J.F., Dong, W., Yuan, B.Y., Li, S.S., Huang, W.W., Liu, Y., Bai, L.Y., Bao, L., Li, S., Yang, J.G., Zhang, L.M., Zhang, Z.J., 2012. The first trial excavation and significance of Wulanmulun site in 2010 at Ordos, Inner Mongolia in north China. Quat. Sci. 32, 178–187 (in Chinese).

Huntley, D.J., Baril, M.R., 1997. The K content of the K-feldspars being measured in optical dating or in thermoluminescence dating. Anc. TL 15, 11–13.

Huntley, D.J., Lamothe, M., 2001. Ubiquity of anomalous fading in K-feldspars and the measurement and correction for it in optical dating. Can. J. Earth Sci. 38, 1093–1106.

Li, B., Li, S.H., 2006. Comparison of D-e estimates using the fast component and the medium component of quartz OSL. Radiat. Meas. 41, 125–136.

Li, B., Li, S.H., 2011. Luminescence dating of K-feldspar from sediments: a protocol without anomalous fading correction. Quat. Geochronol. 6, 468–479.

Li, B., Li, S.-H., 2012. Luminescence dating of Chinese Loess beyond 130 ka using the non-fading signal from K-feldspar. Quat. Geochronol. 10, 24–31.

Li, B., Li, S.H., Wintle, A.G., Zhao, H., 2008. Isochron dating of sediments using luminescence of K-feldspar grains. J. Geophys. Res. Earth Surf. 113, F02026 doi: 02010.01029/02007JF000900.

Li, B., Roberts, R.G., Jacobs, Z., 2013. On the dose dependency of the bleachable and non-bleachable components of IRSL from K-feldspar: improved procedures for luminescence dating of Quaternary sediments. Quat. Geochronol. 17, 1–13.

Li, B., Jacobs, Z., Roberts, R.G., Li, S.-H., 2014a. Review and assessment of the potential of post-IR IRSL dating methods to circumvent the problem of anomalous fading in feldspar luminescence. Geochronometria 41, 178–201.

Li, G.Q., Jin, M., Wen, L.J., Zhao, H., Madsen, D., Liu, X.K., Wu, D., Chen, F.H., 2014b. Quartz and K-feldspar optical dating chronology of eolian sand and lacustrine sequence from the southern Ulan Buh Desert, NW China: implications for reconstructing late Pleistocene environmental evolution. Palaeogeogr. Paleoclimatol. Palaeoecol. 393, 111–121.

Meng, Y.-M., Zhang, J.-F., Qiu, W.-L., Fu, X., Guo, Y.-G., Zhou, L.-P., 2015. Optical dating of the Yellow River terraces in the Mengjin area (China): first results. Quat. Geochronol. 30, 219–225. http://dx.doi.org/10.1016/j.quageo.2015.03.006.

Murray, A.S., Buylaert, J.P., Thomsen, K.J., Jain, M., 2009. The effect of preheating on the IRSL signal from feldspar. Radiat. Meas. 44, 554–559.

Murray, A.S., Funder, S., 2003. Optically stimulated luminescence dating of a Danish Eemian coastal marine deposit: a test of accuracy. Quat. Sci. Rev. 22, 1177–1183.

Prescott, J.R., Hutton, J.T., 1994. Cosmic ray contributions to dose rates for luminescence and ESR dating: large depths and long-term time variations. Radiat. Meas. 23, 497–500.

Qin, J.T., Zhou, L.P., 2012. Effects of thermally transferred signals in the post-IR IRSL SAR protocol. Radiat. Meas. 47, 710–715.

Roberts, H.M., 2012. Testing Post-IR IRSL protocols for minimising fading in feldspars, using Alaskan loess with independent chronological control. Radiat. Meas. 47, 716–724.

Schatz, A.-K., Buylaert, J.-P., Murray, A.S., Stevens, T., Scholten, T., 2012. Establishing a luminescence chronology for a palaeosol-loess profile at Tokaj (Hungary): a comparison of quartz OSL and polymineral IRSL signals. Quat. Geochronol. 10, 68–74.

Schmidt, E.D., Tsukamoto, S., Frechen, M., Murray, A.S., 2014. Elevated temperature IRSL dating of loess sections in the East Eifel region of Germany. Quat. Int. 334, 141–154.

Sohbati, R., Murray, A.S., Buylaert, J.P., Ortuno, M., Cunha, P.P., Masana, E., 2012. Luminescence dating of Pleistocene alluvial sediments affected by the Alhama de Murcia fault (eastern Betics, Spain) – a comparison between OSL, IRSL and post-IR IRSL ages. Boreas 41, 250–262.

Spooner, N.A., 1994. The anomalous fading of infrared-stimulated luminescence from feldspars. Radiat. Meas. 23, 625–632.

Teilhard de Chardin, P., Licent, F., 1924. On the discovery of a Palaeolithic industry in northern China. Bull. Geol. Soc. China 3, 45–50.

Thiel, C., Buylaert, J.P., Murray, A., Terhorst, B., Hofer, I., Tsukamoto, S., Frechen, M., 2011. Luminescence dating of the Stratzing loess profile (Austria) – Testing the potential of an elevated temperature post-IR IRSL protocol. Quat. Int. 234, 23–31.

Thomsen, K.J., Murray, A.S., Jain, M., Botter-Jensen, L., 2008. Laboratory fading rates of various luminescence signals from feldspar-rich sediment extracts. Radiat. Meas. 43, 1474–1486.

Trauerstein, M., Lowick, S.E., Preusser, F., Schlunegger, F., 2014. Small aliquot and single grain IRSL and post-IR IRSL dating of fluvial and alluvial sediments from the Pativilca valley. Peru. Quat. Geochronol. 22, 163–174.

Tsukamoto, S., Murray, A.S., Huot, S., Watanuki, T., Denby, P.M., Botter-Jensen, L., 2007. Luminescence property of volcanic quartz and the use of red isothermal TL for dating tephras. Radiat. Meas. 42, 190–197.

Wang, X.L., Wintle, A.G., 2013. Investigating the contribution of recuperated TL to post-IR IRSL signals in a perthitic feldspar. Radiat. Meas. 49, 82–87.

Wang, X.L., Wintle, A.G., Adarniec, G., 2014. Post-IR IRSL production in perthitic feldspar. Radiat. Meas. 64, 1–8.

Wang, Z.H., Hou, Y.M., Yang, Z.M., Zhen, Z.M., Liu, Y., Bao, L., Yang, J.G., Bai, L.Y., Zhang, L.M., 2012. The wulanmulun paleolithic site in Middle Paleolithic Age in Ordos, inner Mongolia. Archaeology 7, 3–14 (in Chinese).

Wintle, A.G., 1973. Anomalous fading of thermoluminescence in mineral samples. Nature 245, 143–144.

Wintle, A.G., Murray, A.S., 2006. A review of quartz optically stimulated luminescence characteristics and their relevance in single-aliquot regeneration dating protocols. Radiat. Meas. 41, 369–391.

Zhao, H., Li, S.H., 2005. Internal dose rate to K-feldspar grains from radioactive elements other than potassium. Radiat. Meas. 40, 84–93.